ELSEVIER

Marine Geology 175 (2001) 199–219

MARINE GEOLOGY
INTERNATIONAL JOURNAL OF MARINE GEOLOGY, GEOCHEMISTRY AND GEOPHYSICS

www.elsevier.nl/locate/margeo

Laboratory and field evaluations of the LISST-100 instrument for suspended particle size determinations

Jeffrey W. Gartner[a,*], Ralph T. Cheng[a], Pei-Fang Wang[b], Kenneth Richter[b]

[a]*US Geological Survey, Water Resources Division, Menlo Park, CA, USA*
[b]*Marine Environmental Quality Branch, Space and Naval Warfare Systems Center, San Diego, CA, USA*

Received 1 May 2000; accepted 1 February 2001

Abstract

Advances in technology have resulted in a new instrument that is designed for in-situ determination of particle size spectra. Such an instrument that can measure undisturbed particle size distributions is much needed for sediment transport studies. The LISST-100 (Laser In-Situ Scattering and Transmissometry) uses the principle of laser diffraction to obtain the size distribution and volume concentration of suspended material in 32 size classes logarithmically spaced between 1.25 and 250 μm. This paper describes a laboratory evaluation of the ability of LISST-100 to determine particle sizes using suspensions of single size, artificial particles. Findings show the instrument is able to determine particle size to within about 10% with increasing error as particle size increases. The instrument determines volume (or mass) concentration using a volume conversion factor C_v. This volume conversion factor is theoretically a constant. In the laboratory evaluation C_v is found to vary by a factor of about three over the particle size range between 5 and 200 μm. Results from field studies in South San Francisco Bay show that values of mass concentration of suspended marine sediments estimated by LISST-100 agree favorably with estimates from optical backscatterance sensors if an appropriate value of C_v, according to mean size, is used and the assumed average particle (aggregate) density is carefully chosen. Analyses of size distribution of suspended materials in South San Francisco Bay over multiple tide cycles suggest the likelihood of different sources of sediment because of different size characteristics during flood and ebb cycles.

Keywords: Laser in-situ scattering and transmissometry; Particle size distribution; Suspended solids concentration; San Francisco Bay; California

1. Introduction

Critical components of understanding the transport, deposition, and erosion of fine sediments in bays and estuaries include knowledge of the size distribution and mass concentration levels of suspended sediments and how they change over time. Although instruments designed to estimate total concentration of suspended solids have been available for years, no such instrument has been available until recently to allow in-situ measurements of size distributions of suspended material.

The optical backscatterance sensor (OBS) has been widely used since the 1980s to estimate time series of suspended solids concentration (SSC) (Downing et al., 1981). OBS has been used in a wide range of applications on continental shelves, in bays, rivers, and estuaries (Cacchione and Drake, 1990; Kineke and Sternberg, 1992; Schoellhamer, 1996, among others). An OBS emits infrared (IR) light and

* Corresponding author.

0025-3227/01/$ - see front matter
PII: S0025-3227(01)00137-2

measures the IR backscattered from material in a small sampling volume near the IR sensor. Because the backscattered signal depends strongly on the properties of suspended sediments, in order to obtain SSC, the OBS must be calibrated against suspended sediment concentrations from the study site. Errors in SSC estimates will occur if the size distribution, composition, or shapes of suspended materials change during the period of measurement (Downing et al., 1981; Downing and Beach, 1989; Ludwig and Hanes, 1990; Downing, 1996). A more critical limitation is that OBS does not provide any information about the size distribution of suspended materials.

There are methods with which to determine size distribution; they require analysis of water samples collected at study site. These include mechanical sorting methods such as dry and wet sieving, methods which are based on the rate of particle settling, such as pipette, hydrometer, and settling tube, and methods based on the electrical properties of sediment particles in water, such as the Coulter Counter.[1] While these methods are reasonably accurate in determining unconsolidated grain size distribution, they destroy particle aggregates that might be present in-situ. Furthermore, these methods are very labor intensive to use. In addition, some methods may lack resolution or have limits to the size classes that can be measured. Because of intensive labor involved, most experiments tend to under sample, which results in a less than statistically accurate representation of sediment size distribution.

Eisma et al. (1996) presents an inter-comparison of several in-situ methods for measuring suspended material that includes video and still camera imaging techniques. In general, imaging techniques do not modify particle size distributions and have the ability to determine sizes of very large particle flocs on the order of 1000 μm. However, these methods may have limitations in their ability to determine very small particle sizes and these methods usually require analysis of a number of images for reliable size distributions.

There is a class of instrument that uses laser diffraction for measurement of particle size distribution (Hildebrand and Row, 1995) and (McCave et al., 1986). Laser light scattering instruments for particle sizing have existed for some years (for example Malvern particle size analyzer and Coulter LS series instruments). Bale and Morris (1987) describes a prototype submersible system based on the Malvern Model 2200 that measures particle size distributions in 15 size classes between 1.2 and 118 μm or 1.9 and 180 μm (based on laser focal length). When tested in Tamar Estuary, the system required shipboard cables for power, digital control, and data transfer during measurements. In the early 1990s, a completely in-situ version of a laser diffraction instrument (Agrawal and Pottsmith, 1994) was developed and tested. A commercial counterpart, the LISST-100 (Laser In-Situ Scattering and Transmissometry), has been introduced by Sequoia Scientific Inc. (Pottsmith and Bhogal, 1995; Agrawal et al., 1996). The initial version of the LISST-100 utilizes a 5 cm laser path length and measures angular scattering distribution obtained with a series of 32 ring detectors to observe particles in 5–500 μm size range. A newer version, LISST-100B, incorporates algorithm changes to measure particle sizing in 1.25–250 μm size range over 32 logarithmically distributed size classes.

The LISST-100 has been previously evaluated using fairly broad and mixed particle size distributions (1–85 and 2–120 μm) of polystyrene particles (Pottsmith and Bhogal, 1995; Agrawal et al., 1996) and tested in laboratory using natural marine sediments (Traykovski et al., 1999). No evaluation of LISST-100 for measuring narrow size distributions of artificial particles has been reported.

Design goals of LISST-100 are to enable in-situ measurements of sediment particle size distribution and volume concentration of suspended solids. Estimates of volume concentration would be possible if the particle size distribution reported by the instrument is accurate. However, the relations between volume concentration and particle size distribution are not well understood. The objectives of this paper are to evaluate the design goals of LISST-100 by means of a series of laboratory tests and field experiments. The first objective is to evaluate the ability of LISST-100B to measure narrow particle size distributions covering the entire measurable size range of 1.25–250 μm. The second objective is to determine

[1] Any use of trade, product, or firm name is for descriptive purposes only and does not imply endorsement by the US Geological Survey.

relations between the volume conversion and the measured sediment size distribution.

This paper begins with an overview of the LISST-100B instrument including its principle of operation. A laboratory setup was designed to achieve the objectives of this study. The laboratory procedures and experimental techniques are discussed in detail. Results of laboratory experiments are presented which are complemented by the results of a field application of LISST-100B along with the conclusions and recommendations.

2. Description of instrument

The LISST-100B (hereafter referred to only as the LISST-100), with an overall length of 81 cm and diameter of 13 cm, is designed for in-situ measurement of particle size spectra and concentration. The instrument also measures optical transmission, temperature, and pressure. Instrument operation is based on Mie theory (Born and Wolf, 1980), which states that at small forward scattering angles, laser light diffraction by spherical particles is essentially identical to diffraction by an aperture of equal size (Fraunhofer approximation) (Agrawal and Pottsmith, 1994). The theory further states that the refractive index of particles (particle composition) has little or no effect on the distribution of light scattering (Agrawal and Pottsmith, 1994). The LISST-100 measures forward scattered laser light intensity distribution through a 5 cm laser path length utilizing a series of 32 annular ring-detectors that are logarithmically spaced in an angular range of 0.0017–0.34 rad (0.0974–19.48°). This configuration is capable of resolving a particle size range of 1.25–250 μm. In this study, data acquisition and analysis software supplied by the manufacturer is used to convert measurements to particle size distribution. Initially, software provided 64 size classes; the latest version of software (Version 3.20) divides particles into 32 logarithmic size classes. Software Version 3.20 is used for all data analyses in this investigation. Instrument measurements are converted to particle area distribution by a mathematical inverse solution. Unfortunately, the inverse problem for determining particle size distribution from the measured scattered light intensity distribution is mathematically ill-posed; approximate solutions have been constructed and described in detail by Agrawal et al. (1991), Agrawal and Pottsmith (1993) and the method of solution will not be discussed here. Particle volume distribution is estimated by determining the volume in each size class $V_{A,i} = (N_{A,i}d_i)/C_v$ where the area in each size class, $N_{A,i}$ is multiplied by the diameter, d_i, of that size class and then divided by a calibration value, C_v. Although C_v is described as a constant by Agrawal et al. (1996), preliminary results described here indicate that the volume conversion factor depends on the particle size distribution in suspension. The appropriate values of C_v will be determined in a series of laboratory experiments.

3. Laboratory evaluation of LISST-100

A series of experiments was carried out to evaluate the ability of the LISST-100 for measurements of suspended solids size distribution and for determining the volume and mass concentration of suspended solids. A laboratory setup was designed specifically to address these two questions through a series of experiments using suspensions of artificial particles of known size. These spherical particles were polystyrene or other polymer with a density of 1.05 g cm^{-3}. The particle size standards are supplied by Duke Scientific Corporation, which has calibrated these particles by National Institute of Standards and Technology traceable microscopy methods (Duke and Layendecker, 1989). Most of the experiments were carried out using mono-sized microspheres including 5, 10, 20, 50, 100, 140, and 200 μm. All standards are available in an aqueous suspension except the 200 μm, which is available as dry powder. In addition, several broad size distributions were tested and analyzed. These included a 1–35 μm distribution (unknown) of polystyrene microspheres and a 1–40 μm distribution (known) of glass beads (density, 2.45 g cm^{-3}).

3.1. Laboratory experiments

The design principle of the laboratory procedure is to mimic as closely as possible the instrument operational conditions in the field. Therefore, an important consideration is that the experimental setup must allow the full 5 cm laser passage through the test

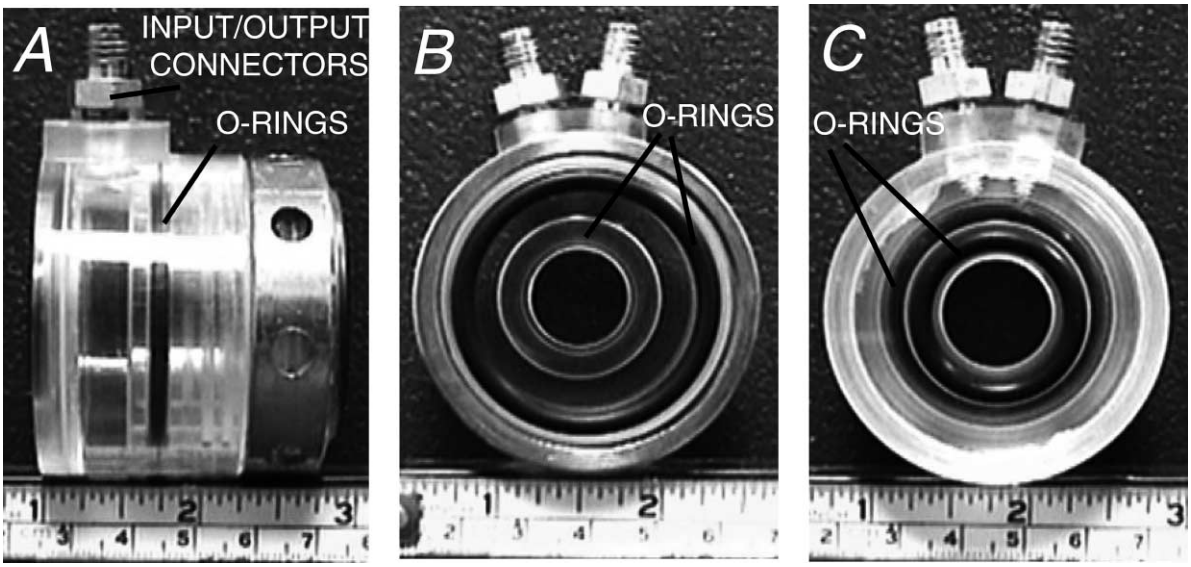

Fig. 1. Test chamber for LISST-100 showing (A) side view, and (B) and (C) end views. End plate O-rings, inflow and outflow connections, and internal O-ring between outer wall of inner tube and inner wall of outer tube are shown.

media and yet keep the required volume of test sample to a minimum as these polystyrene particle standards are very expensive. Within the confines of these requirements, and after testing several versions of test chambers, a test chamber was designed to fit in the region of the LISST-100 where sample volume is located. This test chamber consists of two tightly fitted and adjustable cylinders that fit between endplates with the axis of the cylinders lined up with the laser path of LISST-100. The endplates have holes that correspond to LISST-100 laser and detector windows; O-rings at the end of test-chamber keep it watertight. Inflow and outflow connections on the sidewall allow sample fluid circulation through the test chamber (Fig. 1). When the test chamber is in place, the instrument's laser light is allowed to pass through the entire chamber without obstruction. As shown in Fig. 2, a peristaltic pump is used to keep the test solution circulating between a test solution reservoir (a beaker above a magnetic stirrer) and the test chamber. The continuous circulation keeps particles well mixed and in suspension. This experimental setup virtually mimics the field operational conditions of LISST-100, with the exception that heavy particles tend to settle out in the test chamber because the circulation is not sufficient to keep the particles in suspension. This situation, which could cause some experimental errors, will be discussed further.

Because the test chamber is made of acrylic material, particles are attracted to the chamber sidewalls due to electrostatics. De-ionized (DI) water with 2% sodium hexametaphosphate [$Na_6(PO_3)_6$] was used as a buffer solution to keep the test particles in suspension. The introduction of $Na_6(PO_3)_6$ as a dispersing agent proved to be effective in preventing the polystyrene particles from being attracted to the sides of the test chamber and pump tubing. Since the polystyrene particles have a density of approximately 1.05 g cm^{-3}, a 5% $Na_6(PO_3)_6$ solution by weight (to increase water density) was used for suspensions of larger particles (140 and 200 μm) so that particles were neutrally buoyant during tests.

Each experiment consisted of measuring particle distribution of a known size standard in the test chamber by LISST-100 over a range of concentrations. The experiment started by pumping a known volume of DI water and dispersing agent in the reservoir through the test chamber and back to the reservoir forming a re-circulating system. The instrument background (zero scatter, zscat) was first measured and recorded. After background measurements, the sampling program, which recorded the average of 16 laser scans every 20 s, was initiated. A test particle

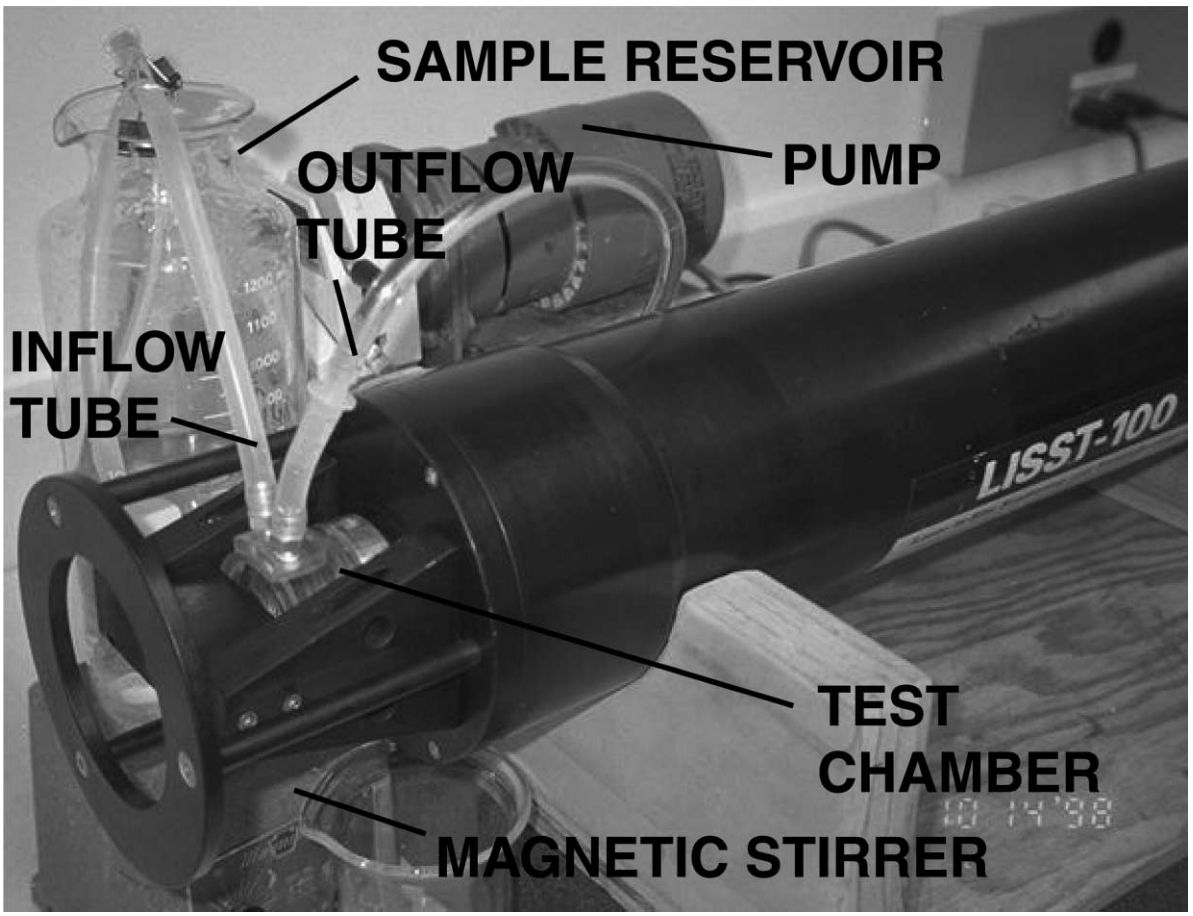

Fig. 2. LISST-100 instrument with laboratory experimental setup showing test chamber installed at region of sample volume. Setup includes magnetic stirrer below the sample beaker. Tubing is used to draw sample from beaker to sample chamber and then to peristaltic pump and back to sample beaker thus closing the loop. Sample concentration is changed by adding liquid to the sample beaker.

suspension consisting of known particle size, mass, and volume of water (DI and dispersing agent) was then added and mixed in the reservoir to produce a new mass concentration of known value. Standard procedures for laboratory chemical operations were followed in making suspension of mono-sized particles available as aqueous suspensions. Potential errors for the procedure come from the precision of the graduated cylinders (listed in supplier catalog) that are less than 1.2%. Precision of measurements of mass (balance specifications) of material supplied as dry particles used in suspensions was less than 2.1%. Concentration levels of the suspensions were kept below levels of multiple scattering (occurring when light transmission measured by the LISST-100 is reduced to about 30%). The pumping rate for circulation was maintained at ≈ 4 ml s^{-1}, which was sufficient to keep particles well mixed and in suspension without generating bubbles in the test chamber. After sufficient measurements for that concentration level were recorded, a known volume of DI water and dispersing agent mixture was added to the reservoir to create a lower concentration level suspension. This process was repeated for five or six concentration levels for each of the particle sizes.

3.2. Laboratory results and analyses

As an example of the experimental technique, measured results of two experiments using 20 and

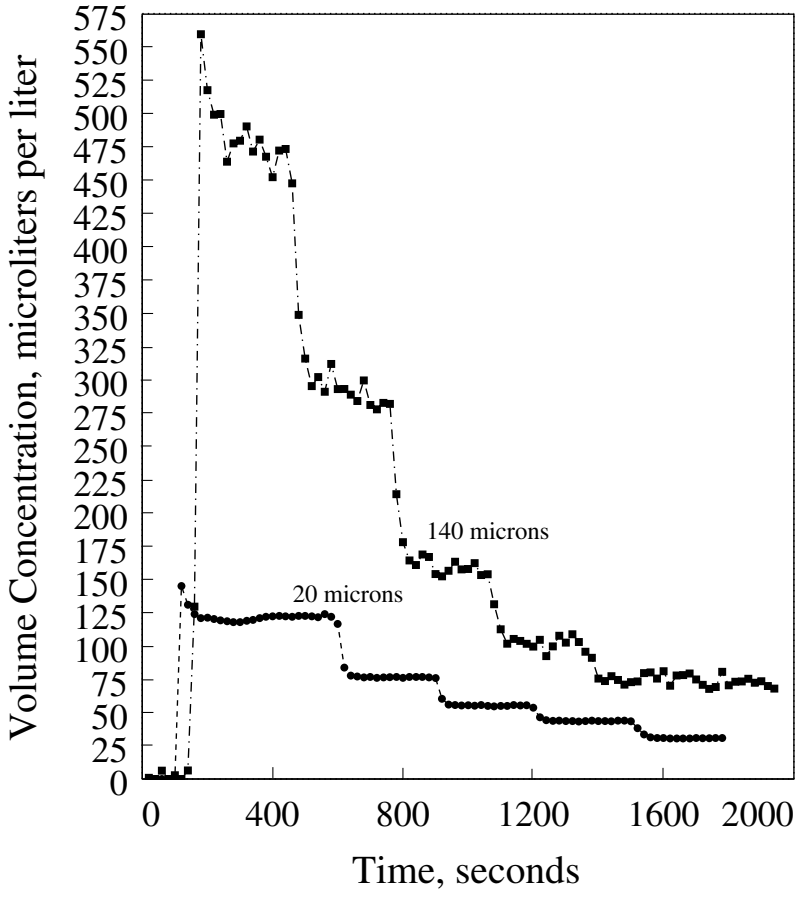

Fig. 3. Time series plots of laboratory test suspensions of 20 and 140 μm particles at five concentration levels. Mass concentrations as determined by LISST-100 were matched to known concentration levels to determine instrument calibration constant.

140 μm polystyrene suspensions are shown in Fig. 3. Volume concentration levels are initially zero, reflecting that only the DI water and dispersing agent are present. After the suspension of particles is introduced into the test chamber, concentration levels increase and stabilize as the suspension circulates through the system. After each dilution, the concentration levels decrease and stabilize to a new, lower level. There are five volume concentration levels shown for each experiment. The time-series plot of the 140 μm particle suspension shows more noise in the measured concentration levels. Even though the concentration levels are higher for the larger particles (140 μm), in order to keep the laser from multiple scattering there are far fewer number of particles in suspension. Both the large particle size and small number of particles tends to make it more difficult to keep the suspension well mixed. In fact, it appears that some particles might be settling out at higher concentration levels, although a clearly defined concentration level can be determined by LISST-100. All particles size standards were examined following these laboratory procedures.

All measurements of particle size distribution were deduced using software provided by the manufacturer (Version 3.2). The volume concentration is also computed by the software and that computation requires a volume conversion factor, C_v. Theoretically, C_v should be independent of particle size distribution. Results of this series of measurements show that C_v could be dependent on particle size. These laboratory test results are discussed in the following Section 3.2.1.

3.2.1. Particle size distribution

Seven mono-sized particle suspensions were used in the experiments; measured results are summarized in Table 1. Column one lists the certified standard particle sizes and their standard deviations supplied by Duke Scientific Corporation. Columns two and three are the LISST-100 measured particle sizes and the respective standard deviations. In general, the LISST-100 successfully determined mean particle size to within 2–18% with increasing error as the test particle size increased. The trend of increasing error with increasing particle size may have resulted, at least in part, from logarithmically spaced instrument detector rings (see Section 3.2.3). Most experiments were re-run with similar results using another LISST-100 unit. Mean sizes measured with the second instrument fell within 1.4% of the certified particle size at 5 μm to 12.7% of the certified particle size at 139 μm (Suspensions of 200 μm particles were not measured with the second instrument).

Among the very few test samples with known particle size distribution is Duke catalog number 414. The nominal particle size distribution ranges between 1–40 μm. Duke #414 consists of glass microspheres with a density of 2.45 g cm^{-3}. A laser Coulter Counter model LS230 was used to analyze this sample independently. Size distributions provided by Duke Scientific Corporation (Coulter $Z_B + H_4$ Channelyzer), the laser Coulter Counter model LS230, as well as those measured by LISST-100 are compared in Fig. 4. Because the number and definition of the size classes are different for each of these three instruments, the volume concentrations are shown as cumulative volume percent for comparison (Fig. 4). Although only one representative graph for each instrument is shown in Fig. 4, the LISST-100 graphs are nearly identical for ten scans (mean particle size, 13.42 μm; standard deviation, 6.83 μm). The graph for the Coulter Model LS230 is one of two replicates (mean particle size, 10.21 μm; standard deviation, 5.29 μm) while the distribution data from the supplier consists of a single data set (mean particle size, 11.35 μm; standard deviation, 1.49 μm). There are some discrepancies among the three measured values at small ($< \approx 5$ μm) sizes; the LISST-100 tends to estimate sizes that fall between the estimates made by the other two methods. Above ≈10 μm, the LISST-100 tends to show cumulative volume percent less than the other two estimates but typically within about 10% of the values provided by the particle supplier. Differences below 5 μm may be the result of different measurement techniques in this particle-size range where Fraunhofer diffraction technique begins to loose applicability because scattered light patterns are less distinct.

3.2.2. Volume concentration estimates

Once the particle size distribution is measured, the volume concentration of suspended particles can be estimated if a volume conversion factor, C_v, is provided to post-processing software. In this series of laboratory experiments, a best-fitting value of C_v was determined for each size class by minimizing the percent difference between the known volume concentration values (fourth column) and LISST-determined volume concentration values (fifth column) in Table 1. The best-fitting C_v for each size class is given in column six along with the sum of percent difference between known and measured volume concentrations. The C_v values are summarized in Fig. 5 based on experiments using two LISST-100s in the laboratory tests. The volume conversion factor, C_v, decreases with increasing particle size for each set of the laboratory tests for the two LISST-100 instruments (Fig. 5). Rather than being independent of particle sizes, the volume conversion factor, C_v, varies over a factor of three inversely proportional to log(size) in the range between 5–200 μm (Fig. 5 and Table 1). Furthermore, the volume conversion factors differ between the two instruments, although the trends are consistent. The reason for this discrepancy might be due to the sensitivities of the instrument detectors, and instrument calibration constants. There is no theoretical reason to explain this variance of the volume conversion factor. Users of LISST need to be aware that the volume conversion factor is an experimentally calibrated value.

3.2.3. Discussion of laboratory experiments

In general, results from these controlled laboratory experiments suggest that the LISST-100s that were evaluated tend to underestimate mean particle size up to about 10–20%, with largest errors in the biggest size classes (Table 1). Since the detector rings in the LISST-100 are logarithmically spaced (the upper size of each bin is 1.18 times the lower size), instrument

Table 1
Analyses of mono-sized particle suspensions measured by LISST-100. There are five or six concentration levels for each particle size (SD = standard deviation)

Duke Scientific Corporation	LISST-100	LISST-100	Test suspension		Conversion constant, C_v
[a]Standard size (μm)	Measured size (μm)	SD (μm)	Suspension concentration (ml l^{-1})	Measured concentration (ml l^{-1})	Total percent difference
4.99 ± 0.04 SD = 0.06	4.5	1.7	31.0	34.4	$C_v = 9000$ [b]$\sum\%\Delta = -0.39$
	4.6	1.6	20.7	21.3	
	4.7	1.4	15.5	15.3	
	4.7	1.4	12.4	11.8	
	4.7	1.3	8.9	8.2	
9.975 ± 0.06 SD = 0.09	10.4	4.3	47.9	44.0	$C_v = 7800$ $\sum\%\Delta = 0.52$
	10.6	4.2	30.3	29.3	
	10.6	4.1	21.9	22.0	
	10.6	4.5	17.1	17.5	
	10.5	3.8	11.7	12.6	
20.00 ± 0.10 SD = 0.20	19.2	6.7	108.5	115.6	$C_v = 6900$ $\sum\%\Delta = 5.02$
	19.5	6.5	72.3	73.0	
	19.6	6.2	54.3	52.7	
	19.7	6.2	43.4	41.6	
	19.9	6.2	31.0	29.3	
50.40 ± 1.0 SD = 1.6	47.4	12.7	105.0	111.3	$C_v = 6300$ $\sum\%\Delta = 1.26$
	47.7	12.3	70.0	70.5	
	47.8	11.8	52.5	51.5	
	47.9	11.8	42.0	40.9	
	47.9	11.5	30.0	29.0	
100.0 ± 2.0 SD = 2.9	90.8	19.0	258.5	220.0	$C_v = 3800$ $\sum\%\Delta = -0.16$
	90.5	18.8	170.8	146.7	
	90.8	18.6	114.9	110.0	
	91.2	18.1	85.2	88.0	
	91.2	17.1	56.4	62.9	
	91.9	15.5	41.2	48.9	
139.0 ± 2.8 SD = 6.5	122.7	25.7	212.7	188.5	$C_v = 3700$ $\sum\%\Delta = 7.39$
	122.7	25.2	132.6	125.7	
	124.5	24.9	100.3	94.3	
	124.2	24.0	73.5	75.4	
	124.8	22.4	47.9	53.9	
200.0 ± 5.8 SD = 5.8	159.6	37.3	234.1	212.8	$C_v = 3100$ $\sum\%\Delta = -4.93$
	162.5	36.5	163.9	152.0	
	163.2	35.6	116.8	118.2	
	166.5	32.4	76.7	81.8	
	172.4	25.9	55.3	62.6	

[a] Certified particle size standards supplied by Duke Scientific Corporation.
[b] Sum of percent difference between known test suspension and measured volume concentration.

resolution becomes poorer with increasing particle size range. For example, the ring that represents a nominal size 5 μm covers 4.70–5.54 μm. At larger size classes, for example, the ring that represents a nominal size 200 μm covers 179.2–211.5 μm. For larger size-classes, the band width (particle size range represented by a detector ring) increases with particle sizes. Suspensions of large mono-sized particles are not well represented by detector rings. Thus, the standard deviations also increase with particle sizes. However, the relative errors (standard deviation divided by the nominal particle size) remain in the

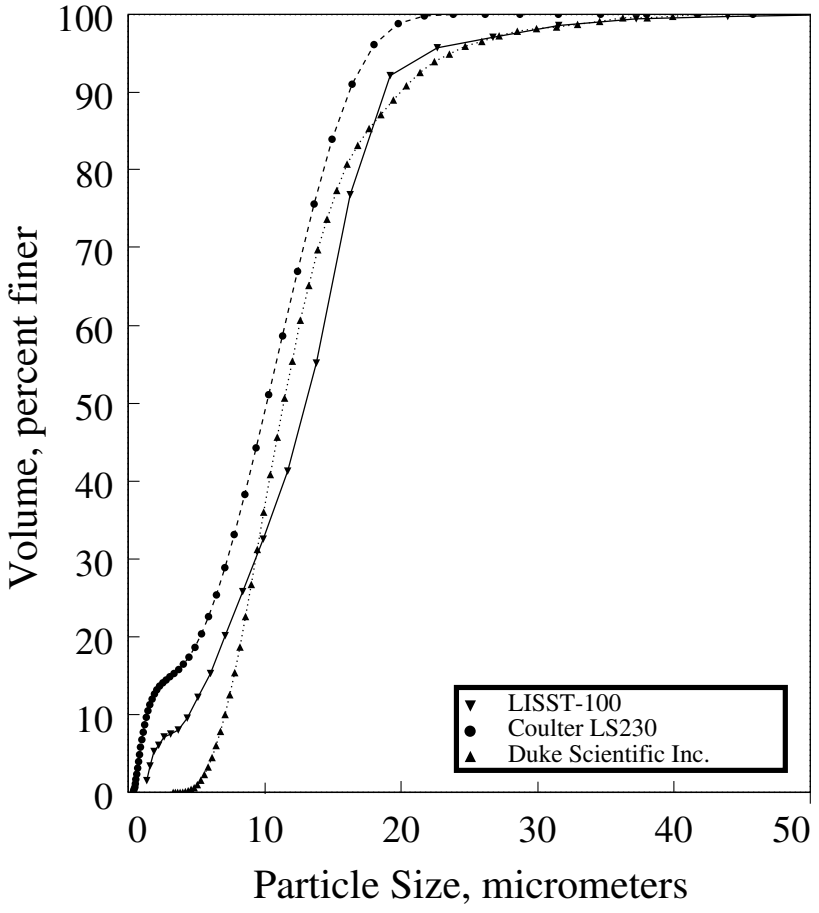

Fig. 4. Comparison of size distributions of suspension of 1–40 μm particles (Duke #414) as determined by LISST-100 (down triangles), laser Coulter® model LS-230 (circles), and Coulter® Counter (Coulter $Z_B + H_4$ Channelyzer) as provided by the supplier, Duke Scientific (up triangles). Size distribution is provided as a volume percent (percent of suspended material in a given size class) because there are a different number and location of size classes for each instrument.

range of 20–30% bias towards under-estimating particle sizes. Interestingly, Traykovski et al. (1999) found that the LISST (5 cm laser path; 2.5–500 μm range) that they evaluated in laboratory with natural marine sediments tended to slightly overestimate the size of sediments. The measured results of LISST are sensitive to the detector rings of each individual instrument. Any improvement in the ring-area file, the set of numerical calibration weighs supplied by the manufacturer and used by the software to adjust the sensitivity of ring detectors, would lead to more accurate determination of particle size distribution.

The dependence of volume conversion factor, C_v, with particle size is in part due to inaccuracy in the measurements of particle size, especially at the larger size classes that carries more weight in the volume concentration estimates. Because the volume concentration depends on the third power of the particle radius, any error in particle size distribution will produce a proportionately larger error in volume concentration. For example, the mean size of 100 μm standard particles measured by the LISST-100 was about 91 μm, an under estimation of 9%. Correspondingly, the volume concentration would be underestimated by about 25% ($1 - 0.91^3$). The volume concentration errors increase with the increasing particle size and decrease with the decreasing particle size. This explains the trend of decreasing

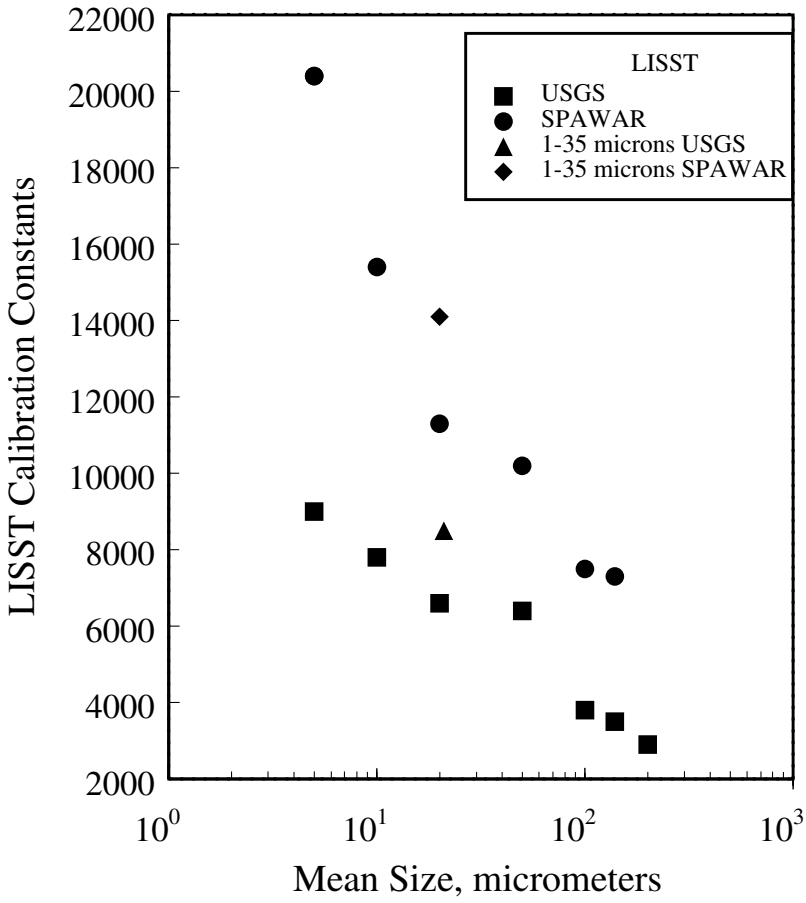

Fig. 5. Calibration constants determined in the laboratory using polystyrene spheres plotted against particle size. Results are from two instruments belonging to the US Geological Survey and the Space and Naval Warfare Systems Center.

C_v with increasing particle size. However, it does not account for all of the differences found for C_v values at different sizes. For particle sizes of 100 μm and larger, the errors in particle size only account for about 25–30% of the error in volume concentration had a constant (average) value of C_v been used for all calculations. In mid range (10–50 μm particles), where an average value of C_v is appropriate, errors from size and constant C_v are similar whereas at 5 μm the errors from size estimate and constant C_v are in opposite directions. Based on this series of laboratory experiments, a volume conversion factor C_v for diameter d particles (in μm) could be given as

$$C_v = (C_v)_{@10}/\log(d) \quad (1)$$

where $(C_v)_{@10}$ is the conversion factor for 10 μm particles. The proposed formula suggests a compensation to volume errors embedded in C_v. Note that the choice of C_v does not affect the size distribution.

A similar series of experiments with the 2nd LISST-100 (labeled SPAWAR in Fig. 5), gives results that show similar trends, although actual values of the measured parameters vary slightly. The differences are probably the result of variance in the sensitivity of laser detectors in each instrument.

4. Field applications of LISST-100

The LISST-100 was designed as a field instrument

to enable in-situ measurements of sediment size distribution as well as SSC. Results of a field deployment of LISST-100 will be discussed. Based on the previously described laboratory experiments, the response of LISST-100 under field conditions can be better understood for interpreting measurements. Results of field measurements are expected to deviate from laboratory results because the characteristics of naturally occurring suspended materials are substantially different in shape, structure, and density from the spherical polystyrene particles used for calibrations in laboratory. Differences between instrument response to particle standards in laboratory and to natural sediment particles in field are examined in the following Section 4.1 and above.

4.1. Field experiment

San Francisco Bay is a complex estuarine system comprising two hydrologically distinct sub-estuaries (Fig. 6): the northern reach, which connects the confluence of the San Joaquin and Sacramento Rivers with the Pacific Ocean at Golden Gate, and South San Francisco Bay (South Bay). The northern reach receives most of the freshwater that enters the bay system. South Bay is considered a semi-enclosed embayment that is generally well mixed except during periods of high local runoff and river discharge. Tides and tidal currents in the bay are mixed diurnal and semidiurnal types, mainly semidiurnal.

As part of an ongoing research program to better understand bottom boundary layer properties and sediment transport, two sites were chosen for deployment of an instrument platform equipped with a variety of instruments to measure hydrodynamic and water quality characteristics in South Bay during October 1998. A suite of instruments including the LISST-100 was first deployed in the main channel just north of the San Mateo Bridge (SMB site) between October 19 and 23, 1998 (Fig. 6). The instruments were later moved to the main channel just south of the Dumbarton Bridge (DB site) between October 23 and 29, 1998. The two locations shared similar hydrodynamic conditions; however, prior studies indicated that size distributions of suspended materials were probably somewhat different at the two sites (Conomos, 1963; Knebel et al., 1977).

In addition to the LISST-100, there were two acoustic Doppler current profilers (ADCPs), four conductivity–temperature–depth (CTD) data loggers, and four OBS sensors. Detailed discussions of data from the ADCPs and CTDs are not included in this paper; they are presented only when they are related to analysis of the LISST-100 and OBS data sets. The LISST-100 was mounted at 220 cm above bed while OBS sensors were mounted at 41, 71, 107 and 220 cm above bed. Unfortunately, the data from the OBS mounted at 220 cm above bed were unusable because of problems with the data logger. The LISST-100 was programmed to record an average of 16 scans (taking about 4 seconds) once every 15 min. The OBS sensors recorded an average of 99 samples (taking less than 1 s) once every 15 min.

4.2. Analysis of field data

Except for the OBS located at 220 cm above bed, all sensors operated successfully at the two deployment sites covering a period from near spring (maximum) to near neap (minimum) tides and tidal currents. LISST-100 data were processed utilizing software provided by the manufacturer to convert the measured scattering intensities to size distribution. The time series of volume concentration was computed using a suitable volume conversion factor based on measured sediment size distribution.

Before instrument deployments, the OBS and LISST-100 were calibrated to estimate total mass concentration utilizing material from the upper few millimeters of grab samples of sediments collected at the two sites. (The user normally does not calibrate the LISST-100 for size distribution.) Bottom sediment material was mixed with bay water in a large bucket and kept in suspension. The instruments were calibrated for SSC by taking measurements and water samples of suspended material in the bucket. Material in the bucket was successively diluted using surficial bay water to provide 4 concentration levels plus a sample of surface water only. These water samples were later filtered and weighed to become the 'ground-truth' sediment concentrations. Comparison of the measured and 'ground truth' data forms the basis for the development of a rating calibration curve for OBS voltage versus concentration. This method of calibration of OBS with bottom sample is subject to possible error if size distribution of bottom

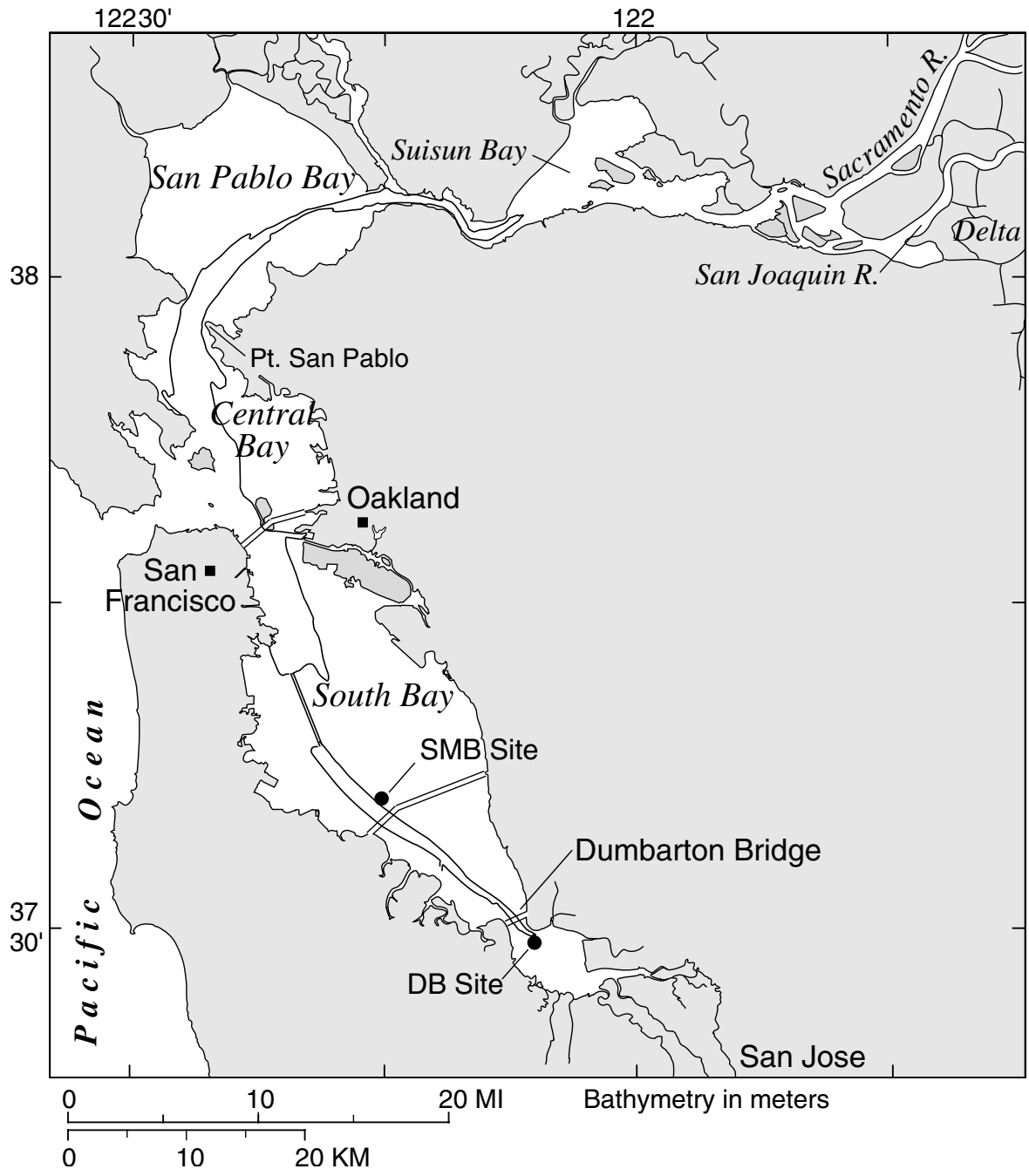

Fig. 6. San Francisco Bay, California showing location of two field sites about 1 km north of the San Mateo Bridge and about 1 km south of the Dumbarton Bridge.

sample varies substantially from that of suspended sediments above bed at the point of OBS measurement. However, because of the highly variable nature of suspended sediments, the procedure of calibrating OBS from water samples collected at the OBS measurement location is also subject to possible errors that can result from collecting an insufficient number of water samples or taking them from the wrong location. Nonetheless, the (successive dilution) technique employed provided successful calibrations of the OBS instruments (output voltage vs. concentration regression where r^2 is in the range of 0.94–0.97).

Unfortunately, concentration levels of these successively diluted water samples generally exceeded the threshold of multiple scattering for the LISST-100. Additionally, the process of mixing and diluting bottom sediments with surface water may change the character of aggregated particles and thus the size distribution and density of suspended material in the water sample used for calibration. Therefore this procedure is generally not useful for calibration of the LISST-100 to determine mass concentration. To estimate mass concentrations of suspended sediment utilizing the LISST-100, measurements are converted to mass concentrations by assuming a volume conversion factor, C_v that is appropriate for the size distribution and an average particle (aggregate) density that is suitable. Mass concentrations determined in this manner can then be compared to estimates of mass concentration from the nearest OBS. However, choice of the assumed particle density is not a trivial issue.

Dry densities of chlorite, kaolinite, illite, and montmorillonite [the primary clay minerals composing suspended sediments in San Francisco Bay (Knebel et al., 1977)] are 2.60–2.90 g cm^{-3}, 2.60–2.65 g cm^{-3}, 2.66 g cm^{-3}, and 2.49 g cm^{-3} respectively. Thus, an average dry density, ρ_d of disaggregated clay minerals is about 2.64 g cm^{-3}. Measurements of disaggregated particle size distributions of suspended sediments in San Francisco Bay have generally been found to be $< \approx 10$ μm (Conomos and Peterson, 1977; Knebel et al., 1977). Kranck and Milligan (1992) found size distribution of disaggregated suspended material in San Pablo Strait (in the northern reach of San Francisco Bay) to be poorly sorted with approximately the same volume in each size class; concentrations fell off rapidly beyond about 10–30 μm.

Dry density, ρ_d does not account for water associated with particle aggregates that make up a substantial portion of suspended material in estuaries where salinities may approach oceanic values; measurements by LISST indicate that most of the suspended material at SMB and DB is probably in the form of aggregates because modal sizes of distributions are larger than 10 μm (see Section 4.2.1). Kranck and Milligan (1992) found in-situ suspended material in San Pablo Strait was well sorted with unimodal size distributions whose modes varied from 101–512 μm. They calculated in-situ, wet density, ρ_{wet} of aggregated materials ranged between 1.032 and 1.270 g cm^{-3} (average 1.077 g cm^{-3}). Krone (1976) estimated ρ_{wet} for aggregated sediments in San Francisco Bay ranged between 1.079 g cm^{-3} and 1.269 g cm^{-3}, with an average value of 1.14 g cm^{-3}.

Defining $\rho_d = M_p/V_p$ where M_p and V_p are the mass and volume of the solid part of the particle and $\rho_{wet} = (M_p + M_w)/(V_p + V_w)$ where M_w and V_w are the mass and volume of aggregate associated water respectively, then an apparent dry density, ρ_a, can be determined for the aggregates defined as $\rho_a = M_p/(V_p + V_w)$, (Gartner and Carder, 1979). Utilizing these definitions, apparent dry density can be given as

$$\rho_a = (\rho_{wet} - \rho_w)/[1 - (\rho_w/\rho_d)], \quad (2)$$

where ρ_w is the density of associated water (≈ 1.02 g cm^{-3}). Utilizing Eq. (2) with an average aggregate wet density of about $\rho_{wet} = 1.14$ g cm^{-3} and an average dry (solid particle) density of about $\rho_d = 2.64$ g cm^{-3} results in an apparent dry density for the aggregate of $\rho_a = 0.19$ g cm^{-3}. This value of apparent dry density is used to calculate the estimates of mass concentration by LISST-100 that are presented in Section 4.2.2 and Fig. 7.

4.2.1. Sediment size distribution

Difficulties of determining size distribution of naturally occurring suspended solids without destroying particle aggregates or flocs that might be present are well known (Gibbs, 1981, 1982a, b; Gibbs and Konwar, 1982, 1983). A major advantage of LISST-100 over traditional methods for estimating size distribution of suspended solids is its ability to make such measurements in-situ without the need to pump, store, transport, or otherwise handle water samples. Thus the

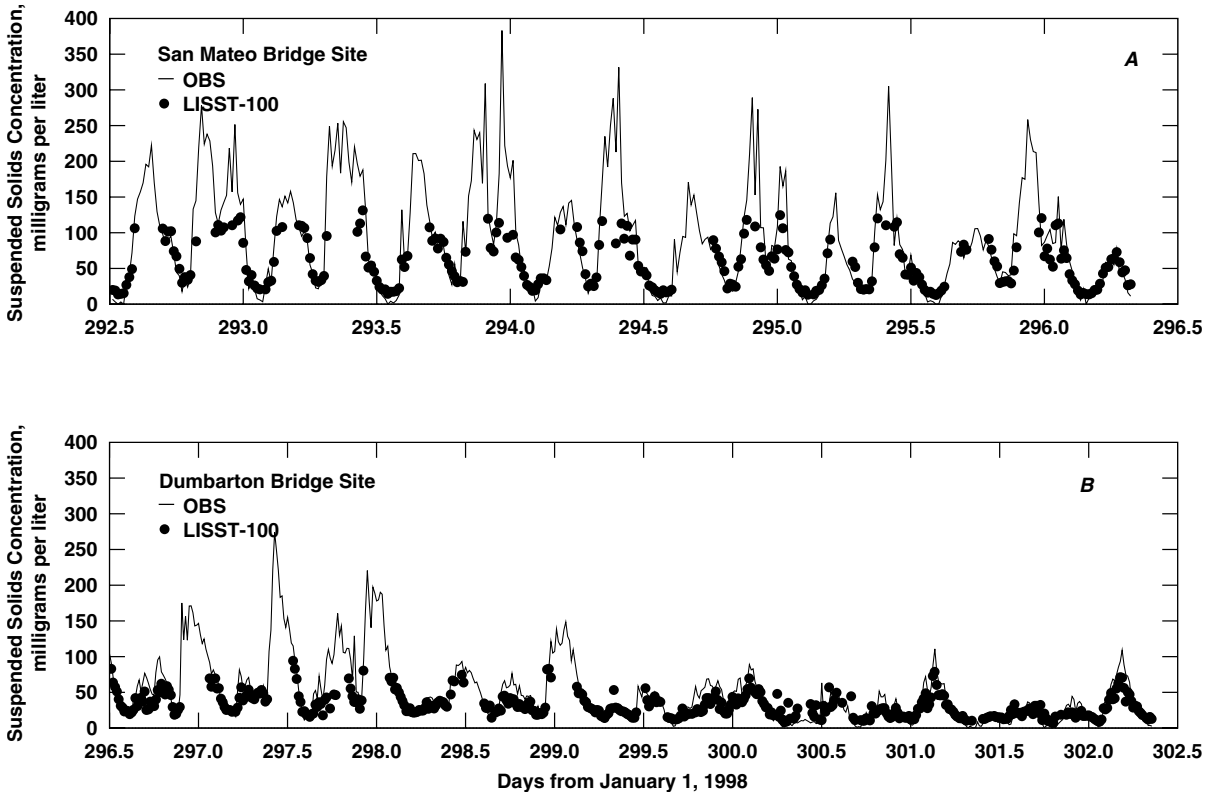

Fig. 7. Time-series plots of SSC estimated by the LISST-100 and the OBS instruments. Estimates from the LISST-100 are truncated above about 100–150 mg l^{-1} when concentration levels resulted in percent transmission less than 20%.

structures of sediment or sediment aggregates tend to remain intact.

General hydrodynamic conditions and in-situ measurements of size distribution made by the LISST-100 from 10/19/98 to 10/23/98 at the SMB site are shown in Fig. 8A–F and at the DB site are shown in Fig. 9A–F. Size distribution near some of the maximum flood currents cannot be determined because concentration levels exceed the threshold of multiple scattering. Multiple scattering becomes increasingly significant as optical transmission falls below about 30%; as optical transmission falls significantly below 10% the estimated size distribution may be biased to smaller sizes (Agrawal, written communication). Thus mean particle sizes are not shown when concentration levels increase to the point that percent transmission measured by the LISST-100 falls below 20%. Use of the LISST-100 is possible in high-concentration regimes if the laser path length is shortened by use of a custom instrument or optically clear plug to reduce sample volume (laser path length).

There are significant differences between the measured suspended sediment properties at the two stations. The mean particle or aggregate size is ≈60 μm and the range in the mean size spans from ≈40 to ≈70 μm at SMB (Fig. 8D), whereas at DB the mean particle or aggregate size is ≈ 50 μm and the range in the mean size spans from ≈30 to ≈70 μm (Fig. 9D). At both SMB and DB, the mean size is generally largest near slack water and smallest near maximum current (usually smaller near maximum ebb than maximum flood). In addition, the shape of the size distribution is quite different at the two sites (Fig. 10). Discounting a very small peak at about ≈ 2 μm that may be real or the result of instrument ring detector calibration inaccuracies, the size distribution at SMB has a single, large peak at ≈ 85–140 μm. The distribution at DB is bimodal; in addition to a

small peak at 2 μm similar to the one at SMB, there are two distinctive peaks at ≈ 20 μm and at ≈ 85–100 μm (The peak at ≈ 20 μm may represent disaggregated particles or some combination of aggregated and single particles). These peaks in the bimodal distribution are separated by about 2–2.5 ϕ which exceeds the minimum resolution limit of the LISST of at least 1 ϕ (Traykovski et al., 1999).

In order to examine how changes in the size distribution of suspended material are correlated with tides and tidal currents (Figs. 8A,B and 9A,B), time-series plots of the percent-suspended solids between 17.7–20.9 μm (nominal 20 μm; LISST size class 17) and between 92.9–109.6 μm (nominal 100 μm; LISST size class 27) are shown in Figs. 8E and 9E. These LISST size classes correspond to the peaks in the size distributions shown in Fig. 10. For clarity, the ratio of the volume concentration at size 100 μm to that at size 20 μm is shown in Figs. 8F and 9F.

At SMB where the size distribution has a single peak, the particle size fraction ratio is almost always greater than two; the large size fraction makes up a higher percent of the total than does the small size fraction. At maximum flood currents the ratio of size fraction increases; at slack water the ratio decreases when the small size fraction makes up a slightly higher percentage of the total. These properties can also be seen in the plot of mean particle size (Fig. 8D) that shows a shift to larger particles during flood currents and smaller particles during ebb currents.

At DB, which has a bi-modal size distribution, the relation between the large size fraction and small size fraction is much different from that at SMB. The small size fraction increases during maximum ebb currents and exceeds the large size fraction for substantial periods (Fig. 9E). This can also be seen in the plot of particle size ratio (Fig. 9F). In general, the size fraction ratio is less than one; there are a higher percentage of finer particles. However, the size fraction ratio can be greater than one for some flood cycles. During flood currents the percent of small particles is similar to the percent of large particles. This is also seen in Fig. 9D which shows mean particle size during flood currents exceeds mean particle size during ebb currents by about 40 μm.

The patterns of size distribution at SMB and DB are probably a result of the combination of several factors including increased suspended loads at maximum currents, different sources of suspended materials during ebb and flood currents, and changes in the amount of aggregated particles due to changes in current speed. Knebel et al. (1977) found differences in clay-mineral content between suspended sediments and bottom sediments in San Francisco Bay that supports the idea that the source of suspended sediments may vary over the tidal cycle. Spatial variation in bottom sediments (see Conomos, 1963) is a possible explanation for an increase in smaller size suspended sediments with ebb currents especially at DB and an increase in larger size suspended sediments with flood currents especially at SMB. It is also possible that the shift to smaller size particles near time of maximum current speeds and the shift to larger size particles near slack water may be explained by the presence of particle aggregates that are broken apart during periods of high tidal energy but begin to reform as slack water approaches.

4.2.2. Suspended solids concentration

Estimation of mass concentration of suspended solids by LISST-100 requires presumptions of values for the volume conversion factor, C_v, and particle density. Since these parameters depend on the degree of particle aggregation, densities of aggregated and disaggregated particles, and size distribution, there is potential for error in estimates of the mass concentration without reliable and appropriate calibration. Based on size distributions at SMB and DB sites (Figs. 8D and 9D, and Table 1), a volume conversion factor, $C_v = 6000$ is used to estimate volume concentration and an apparent dry density value 0.19 g cm^{-3} is used in the process of converting LISST measurements to mass concentration values.

Time-series plots of mass concentration of suspended solids as estimated by an OBS and by the LISST-100 are shown in Fig. 7A and B. Estimates from the two instruments correlate very well, except the mass concentration estimates from the LISST-100 are generally missing during time of peak concentrations (above about 100–150 mg l^{-1}) because percent transmission was too low e.g. at days 293.3 and 294.0 (Fig. 7A) and at days 297.0 and 297.5 (Fig. 7B). Values of LISST-100 measurements are not shown when percent transmission was <20%. Mass concentration levels of suspended solids varied from near

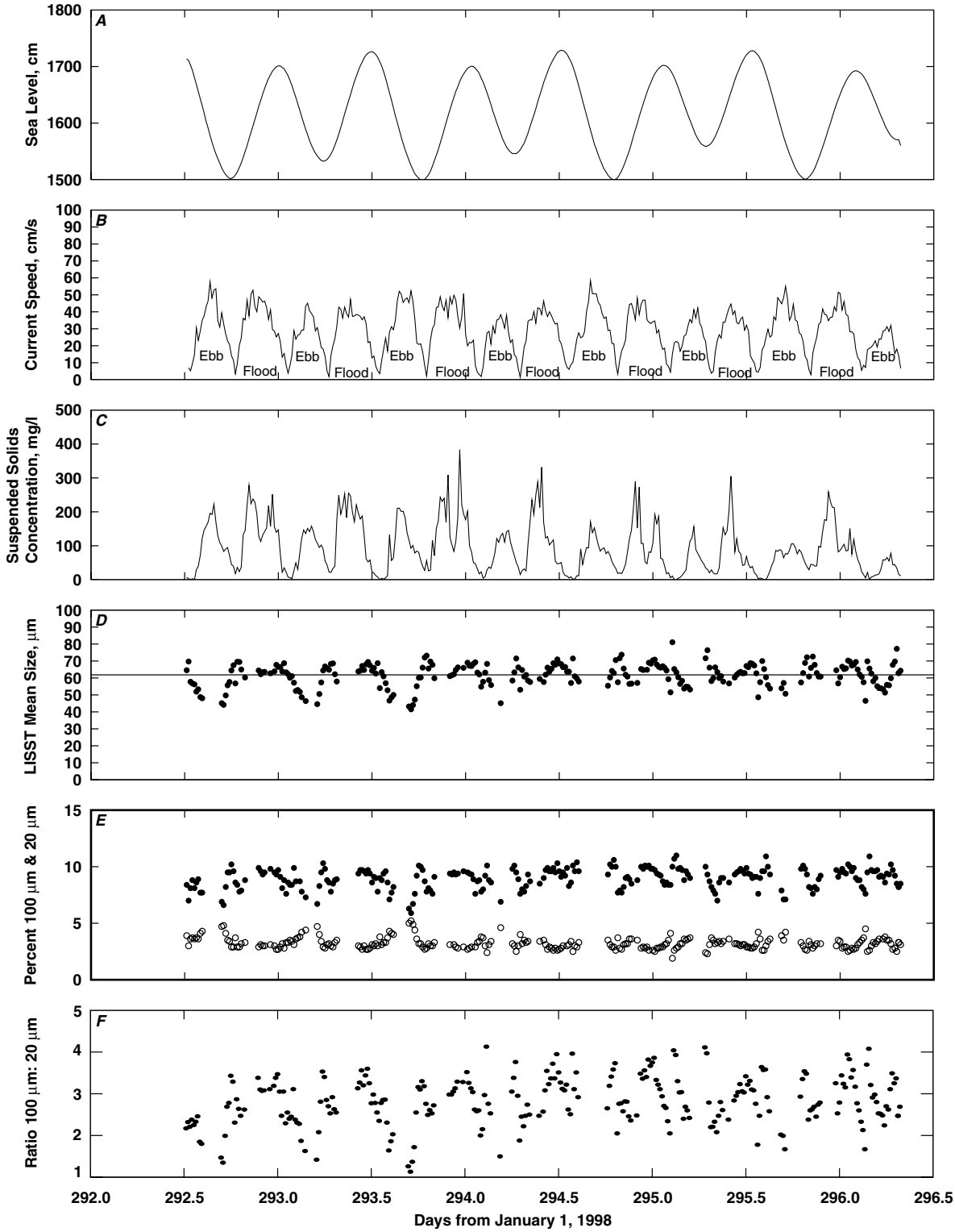
A
Sea Level, cm
1800
1700
1600
1500
B
Current Speed, cm/s
100
90
80
70
60
50
40
30
20
10
0
Ebb
Flood
C
Suspended Solids Concentration, mg/l
500
400
300
200
100
0
D
LISST Mean Size, μm
E
Percent 100 μm & 20 μm
15
10
5
0
F
Ratio 100 μm: 20 μm
5
4
3
2
1
292.0
292.5
293.0
293.5
294.0
294.5
295.0
295.5
296.0
296.5
Days from January 1, 1998

zero mg l^{-1} near slack water to about 200–300 mg l^{-1} near maximum currents. In general, concentration levels were lower at slack after flood than at slack after ebb and concentration levels were higher near maximum flood than near maximum ebb. These patterns held true at both SMB and DB sites.

4.2.3. Discussions of field experiment

No independent measurements of size distribution of suspended solids were made during the deployment of the LISST-100 in South San Francisco Bay. Nevertheless, size distributions of suspended materials measured by the LISST-100 tended to fall in the range of historical measurements from San Francisco Bay (Knebel et al., 1977; Sternberg et al., 1986; Kranck and Milligan, 1992). Underestimates of mean particle size in laboratory measurements are probably not a significant factor in these field measurements because sediment size distribution in field generally fell in regions where errors seen in the lab were small ($\approx 5\%$ at 50 μm). However, because flocculation of suspended material may produce aggregates in the hundreds of μm–mm size range in estuaries (Eisma, 1986), the LISST instrument (size range 1.25–250 μm) may not sample the entire size spectrum present in the bay. For example, Kranck and Milligan (1992) found flocs at a different location in San Francisco Bay with modal sizes between 100 and 500 μm. In addition, the effect of large, aggregated particles as well as non-spherical individual particles is unknown on the determination of size distribution since the LISST-100 assumes solid spherical particles.

Mass concentrations estimated by LISST-100 tracked well with estimates made by OBS. However, mass concentration level above ≈ 150 mg l^{-1} exceeded the limit of LISST-100 for estimates of SSC. This is similar to results seen by Traykovski et al. (1999) for suspended marine sediment in the 5–25 μm size range but is somewhat lower than the concentration of 500 mg l^{-1} where they found multiple scattering occurred for the 25–65 μm size range. While the mean particle sizes were about 50–60 μm at the two locations in San Francisco Bay, a substantial portion of the suspended material falls in smaller sizes especially at the Dumbarton Bridge site (Fig. 10). Unfortunately, concentration levels in South San Francisco Bay often exceed the threshold for multiple scattering beyond which the LISST-100 is unable make reliable measurements in its present configuration.

Some differences in estimates of mass concentration by OBS and LISST-100 may be the result of erroneous calibration of OBS, inaccuracies in assumed density of suspended material, and uncertainty in the volume conversion factor for clay particles found in nature. While the instrument is insensitive to refractive index of particles (Agrawal et al., 1996), laser diffraction instruments are based on Mie scattering theory that assumes spherical particles. Unlike the spherical polystyrene particles, clay minerals, a major component of the suspended sediments in South San Francisco Bay, can be described as flakes, curls, and laths (montmorillonite/smectite); flat particles (chlorite); tabular or glomerular shaped (kaolinite); or irregular edged, tabular shaped (illite/muscovite) (Chamley, 1989). The difference in volume between a spherical particle and a tabular flake-like particle of similar diameter might account for some difference in volume conversion constants determined for laboratory and for field suspensions.

5. Summary and conclusions

Laboratory experiments show that the LISST-100 can be evaluated utilizing a pumping system that incorporates a test chamber to minimize sample volume (and therefore the amount of expensive particle sample), yet still utilizes the full laser path length of the instrument. Laboratory tests show that the instrument underestimates the size of mono-sized particles by about 10%. Errors tended to increase as

Fig. 8. Time series plots of (A) water level; (B) current speed; (C) SSC measured by OBS; (D) mean particle size of suspended material (horizontal line represents deployment mean equal to 62 μm); (E) percent suspended material, 20 μm size class (open circle) and percent suspended material, 100 μm size class (filled circle), and (F) ratio percent suspended material, 20 μm size class to percent suspended material, 100 μm size class at the San Mateo Bridge site. The plots are for the period 10/19/98 (day 292)–10/23/98 (day 296).

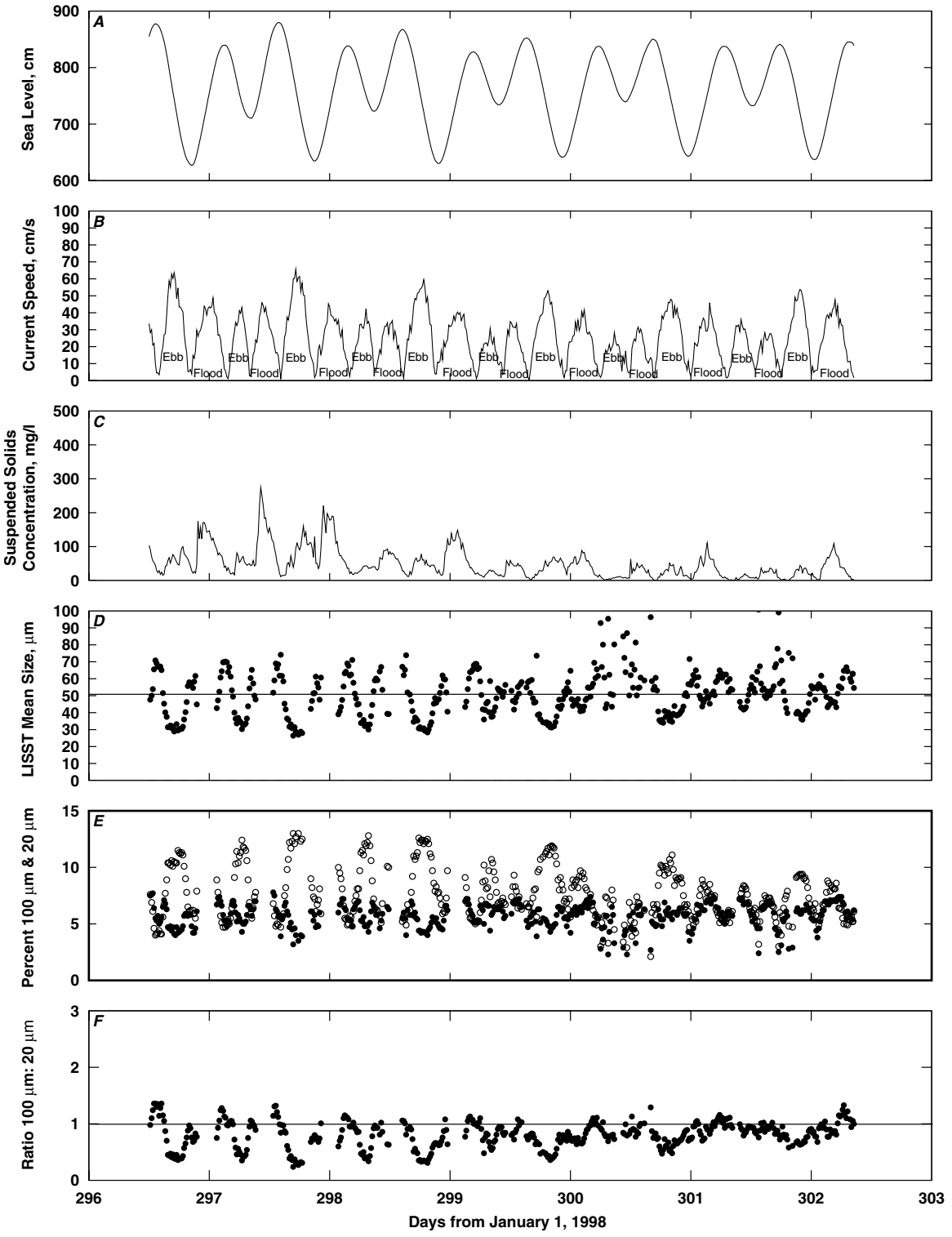
A
Sea Level, cm
900
800
700
600
B
Current Speed, cm/s
100
90
80
70
60
50
40
30
20
10
0
Ebb
Flood
C
Suspended Solids Concentration, mg/l
500
400
300
200
100
0
D
LISST Mean Size, μm
E
Percent 100 μm & 20 μm
15
10
5
0
F
Ratio 100 μm: 20 μm
3
2
1
0
296
297
298
299
300
301
302
303
Days from January 1, 1998

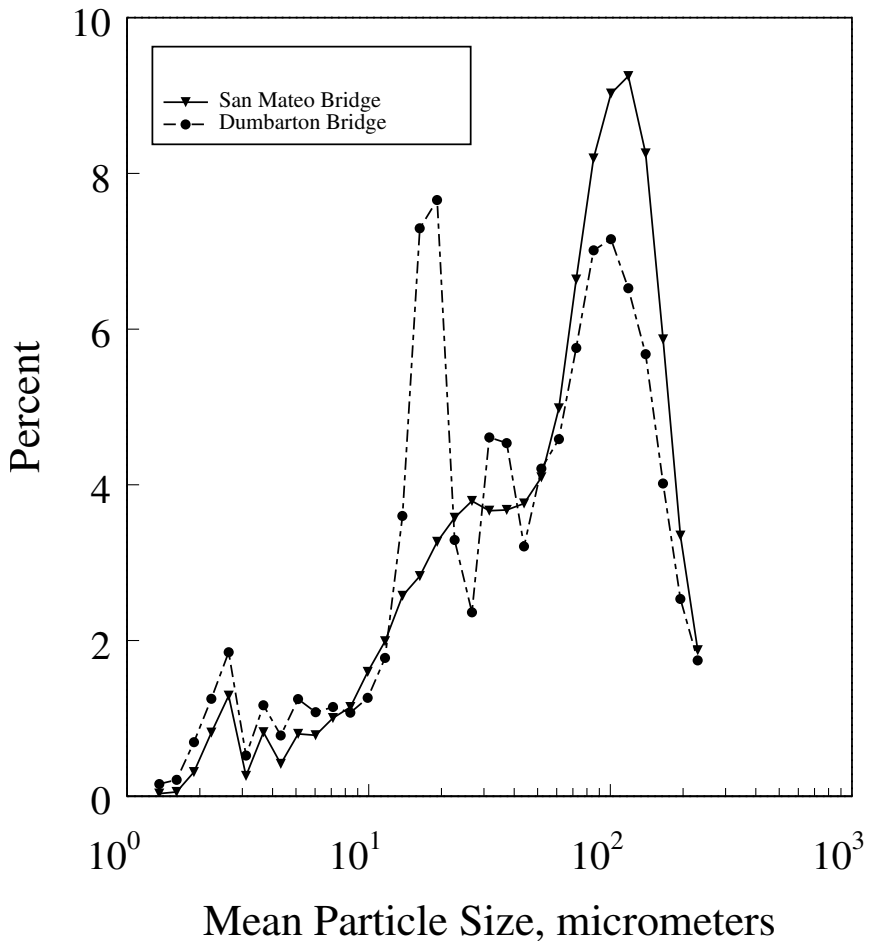

Fig. 10. Plots showing mean size distribution determined by LISST-100 (32 size classes) at San Mateo Bridge site from 10/19/98 to 10/23/98 and at Dumbarton Bridge site from 10/23/98 to 10/29/98.

particle size increased at least in part because the instrument detector rings are logarithmically spaced, thus large mono-sized particles are not well represented by detector rings. Individual instrument detector rings are unique and calibration values are used to adjust sensitivity of detector values. Refined ring detector calibrations would probably improve size estimates.

Estimate of volume (or mass) concentration from particle size distribution depends upon choice of an appropriate volume conversion factor, C_v. Although the volume conversion factor is theoretically constant, laboratory results indicate that it varies inversely with size. Based on mean particle size and laboratory results, a best estimate value of $C_v = 6000$ has been used along with an estimate of apparent dry density of aggregate particles to compute time series of total suspended mass concentration for a field deployment of the LISST-100. Small differences may result from inaccurate estimates of particle density and structural differences between marine particles and aggregates

Fig. 9. Time series plots of (A) water level; (B) current speed; (C) SSC measured by OBS; (D) mean particle size of suspended material (horizontal line represents deployment mean equal to 50 μm); (E) percent suspended material, 20 μm size class (open circle) and percent suspended material, 100 μm size class (filled circle), and (F) ratio percent suspended material, 20 μm size class to percent suspended material, 100 μm size class at the Dumbarton Bridge site. The plots are for the period 10/23/98 (day 296)–10/29/98 (day 302).

seen in the field and solid spherical particles used in the laboratory experiments. Although temporal variations of particle size distribution suggest C_v might also vary with time, generally small size changes that occur within the wide, and often complex, size distributions that are present in natural systems probably do not affect the choice of C_v significantly. However, determining the appropriate apparent particle density is of major importance in determining mass concentration. Suitably calibrated, the LISST-100 should be able to provide estimates of SSC of similar accuracy when compared to estimates provided by OBSs.

Field measurements with the LISST-100 provide insight about the suspended materials at two locations in South San Francisco Bay. Suspended material at the DB site is generally smaller and covers a wider range of sizes than suspended material at the SMB site. Additionally, unlike the SMB site, suspended material at DB has a bi-modal size distribution. Both sites show changes over tidal cycles that include the increased presence of smaller particles on ebb (from south) and increased presence of larger particles on flood (from north). Portions of LISST record at both stations are not valid because transmission fell below 20% (generally at times of maximum flood or ebb). The manufacturer has addressed the threshold limit problem of instrument in high concentration regimes by suggesting that a shortened laser path length be used.

In summary, laboratory and field measurements indicate the potential of the LISST-100 as a powerful research tool in studies of sediment dynamics. Instrument limitations such as the size-dependent volume conversion factor and inability to operate in high concentration regimes are outweighed by the ability to estimate size distribution in-situ without disturbing natural particles and aggregates. The instrument is capable of determining size distribution and volume concentration within acceptable limits. While satisfying, the close agreement between LISST-100 and OBS estimates of mass concentration depends on successfully estimating an average apparent dry density for suspended material, a task that is often difficult at best.

Acknowledgements

The authors would like to thank Fred Murphy of USGS for fabricating the test chambers used in laboratory experiments. Yogi Agrawal, Dave Schoellhamer and two anonymous reviewers provided many valuable comments about the manuscript. As always, Byron Richards and Scott Conard, Captain and Engineer of the R/V Polaris, helped to make the field work enjoyable and successful.

References

Agrawal, Y.C., Pottsmith, H.C., 1993. Optimizing the kernal for laser diffraction particle sizing. Appl. Opt. 32, 4285–4286.

Agrawal, Y.C., Pottsmith, H.C., 1994. Laser diffraction particle sizing in STRESS. Con. Shelf Res. 14, 1101–1121.

Agrawal, Y.C., McCave, I.N., Riley, J.B., 1991. Laser diffraction size analysis. In: Syvitski, J.M. (Ed.), Principles, Methods, and Application of Particle Size Analysis. Cambridge University Press, Cambridge, pp. 119–128.

Agrawal, Y.C., Pottsmith, H.C., Lynch, J., Irish, J., 1996. Laser instruments for particle size and settling velocity measurements in the coastal zone. In: Oceans 1996, Institute of Electrical and Electronic Engineers.

Bale, A.J., Morris, A.W., 1987. In-situ measurements of particle size in estuarine waters. Estuarine Coastal Shelf Sci. 24, 253–263.

Born, M., Wolf, E., 1980. Principles of Optics. 6th ed. Pergamon, Oxford.

Cacchione, D.A., Drake, D.E., 1990. Shelf sediment transport: an overview with applications to the northern California continental shelf, vol. 9. Wiley, New York, pp. 729–773.

Chamley, H., 1989. Clay Sedimentology. Springer, Berlin.

Conomos, T.J., 1963. Geologic aspects of the recent sediments of South San Francisco Bay, Master of Science Thesis, San Jose State College, San Jose, CA.

Conomos, T.J., Peterson, D.H., 1977. Suspended-particle transport and circulation in San Francisco Bay, California: an overview. In: Wiley, M. (Ed.), Circulation, Sediment and Transfer of Material in the Estuary. Estuarine Processes, vol. II. Academic, San Diego, pp. 82–97.

Downing, J.P., 1996. Suspended sediment and turbidity measurements in streams: what they do and do not mean. Presented at the Automatic Water Quality Monitoring Workshop, February 12–13, 1996, Richmond, BC, Canada.

Downing, J.P., Beach, R.A., 1989. Laboratory apparatus for calibrating optical suspended solids sensors. Mar. Geol. 86, 243–249.

Downing, J.P., Sternberg, R.W., Lister, C.R.B., 1981. New instrumentation for the investigation of sediment suspension processes in the shallow marine environment. Mar. Geol. 42, 19–34.

Duke, S.D., Layendecker, E.B., 1989. Improved array method for size calibration of monodisperse spherical particles by optical microscope. Particulate Sci. Technol. 7, 209–216.

Eisma, D., 1986. Flocculation and de-flocculation of suspended matter in estuaries. Neth. J. Sea Res. 20, 183–199.

Eisma, D., Bale, A.J., Dearnaley, M.P., Fennessy, M.J.,

Van Leussen, W., Maldiney, M.-A., Pfeiffer, A., Wells, J.T., 1996. Intercomparison of in-situ suspended matter (floc) size measurements. J. Sea Res. 36 (1–2), 3–14.

Gartner, J.W., Carder, K.L., 1979. A method to determine specific gravity of suspended particles using an electronic particle counter. J. Sed. Petrol. 49, 631–633.

Gibbs, R.J., 1981. Floc breakage by pumps. J. Sed. Petrol. 51, 670–672.

Gibbs, R.J., 1982a. Floc stability during Coulter-Counter size analysis. J. Sed. Petrol. 52, 657–660.

Gibbs, R.J., 1982b. Floc breakage during HIAC light-blocking analysis. Environ. Sci. Technol. 16, 298–299.

Gibbs, R.J., Konwar, L.N., 1982. Effect of pipetting on mineral flocs. Environ. Sci. Technol. 16, 119–121.

Gibbs, R.J., Konwar, L.N., 1983. Sampling of mineral flocs using Niskin bottles. Environ. Sci. Technol. 17, 374–375.

Hildebrand, H., Row, G., 1995. Laser light scattering in particle size analysis. Am. Ceram. Soc. Bull. 74, 49–52.

Kineke, G.C., Sternberg, R.W., 1992. Measurement of high concentration suspended sediments using the optical backscatterance sensor. Mar. Geol. 108, 253–258.

Knebel, H.J., Conomos, T.J., Commeau, J.A., 1977. Clay-mineral variability in the suspended sediments of the San Francisco Bay system, California. J. Sed. Petrol. 47, 229–236.

Kranck, K., Milligan, T.G., 1992. Characteristics of suspended particles at an 11-hour anchor station in San Francisco Bay, California. J. Geophys. Res. 97, 11373–11383.

Krone, R.B., 1976. Engineering interest in the benthic boundary layer. In: McCave, I.N. (Ed.), The Benthic Boundary Layer. Plenum Press, New York, pp. 143–156.

Ludwig, K.A., Hanes, D.M., 1990. A laboratory evaluation of optical backscatterance suspended solids sensors exposed to sand–mud mixtures. Mar. Geol. 94, 173–179.

McCave, I.N., Bryant, R.J., Cook, H.F., Coughanowr, C.A., 1986. Evaluation of a laser-diffraction-size analyzer for use with natural sediments. J. Sed. Petrol. 56, 561–564.

Pottsmith, H.C., Bhogal, V.K., 1995. In situ particle size distribution in the aquatic environment. Paper presented at 14th World Dredging Congress, November 1995, Amsterdam, The Netherlands.

Schoellhamer, D.H., 1996. Factors affecting suspended-solids concentrations in South San Francisco Bay, California. J. Geophys. Res. 101, 12087–12095.

Sternberg, R.W., Cacchione, D.A., Drake, D.E., Kranck, K., 1986. Suspended sediment transport in an estuarine tidal channel within San Francisco Bay, California. Mar. Geol. 71, 237–258.

Traykovski, P., Latter, R.J., Irish, J.D., 1999. A laboratory evaluation of the laser in situ scattering and transmissometry instrument using natural sediments. Mar. Geol. 159, 355–367.